

## Thermal structure of large central European cities using remotely sensed data

R. PONGRÁCZ, J. BARTHOLY and ZS. DEZSŐ

Department of Meteorology, Eötvös Loránd University, Budapest, Hungary  
(e-mail: prita@nimbus.elte.hu, bari@ludens.elte.hu, tante@nimbus.elte.hu)

**Abstract** Part of the NASA's Earth Observing System satellites Terra and Aqua were launched to polar orbit in 1999 and 2002, respectively. Regular measurements are available from July 2000 and July 2002, respectively. Measurements of one of the satellite sensors of the on-board instruments, namely, the Moderate Resolution Imaging Spectroradiometer (MODIS), are used to analyze and compare surface temperature of urban areas in Central Europe (Bucuresti, Budapest, Warsawa, Vienna, Milan, Munich, Sofia, Beograd, Zagreb). MODIS is capable of viewing the entire globe daily with 1 km spatial resolution. Our results suggest that the detected monthly mean urban heat island (UHI) intensities are between 1°C and 6°C, and the most intense UHI occurs in daytime in the summer period.

**Key words:** *urban heat island, surface temperature, sensor MODIS, satellite imagery*

### 1. Introduction

Human settlements and especially, large urban areas significantly modify the environment. Atmospheric composition near urban agglomerations is highly affected mainly due to industrial activity and road traffic. Urban smog events are unfortunate common characteristics of large, very populated cities (Sokhi, 1998). Furthermore, artificial covers (i.e., concrete, asphalt) considerably modifies the energy budget of urban regions, and thus, local climatic conditions. One of the most often analyzed phenomena related to cities is the urban heat island (UHI) effect (e.g., Sundborg, 1950; Oke, 1982). Besides several detailed studies of UHI using ground based measurements (Unger et al., 2001), a more effective tool became available with the use of satellite imagery detected by different sensors on board. The early studies evaluated coarse resolution (7-8 km per pixel) satellite data (Rao, 1972), and the applied methods to calculate surface temperature from spectral observations were very simple (Carlson et al., 1977; Price 1979). These investigations

in the 1970s and 1980s concluded that satellite measurements can be applied to detect the UHI effect in case of clear conditions. The thermal differences between urban and rural areas appear even in case of relatively small towns (Matson et al., 1978). Traditionally, UHI analysis (Howard, 1833; Oke, 1973) uses air temperature data observed at standard height (1.5-2 m above the ground), while satellite images provide thermal information at ground-level. On the base of observed air temperature data, the maximum UHI intensity occurs a few hours after sunset, while the most intense UHI can be detected during day-time when remotely sensed data are used (Roth et al., 1989; Dezső et al., 2005).

In this paper, UHI effects of large cities located in Central Europe are analyzed and compared based on remotely sensed thermal information using 1-km spatial resolution. Section 2 presents the satellite-based time series and the methodology used in this analysis. Then, after discussing the results in section 3, section 4 summarizes the main conclusions of this paper.

## 2. Data and methodology

As part of the Earth Observing System Program of the American National Aeronautics and Space Administration (NASA) satellites Terra and Aqua were launched in December 1999 and May 2002, respectively. Satellite Terra is on a descending orbit (10.30 a.m.), while satellite Aqua is on an ascending orbit (1.30 p.m.), both at 705 km height above the surface. The main goal of remote measurements of these missions is to improve our understanding of global dynamics and processes occurring on the land, in the oceans, the cryosphere, and in the lower atmosphere (NASA 1999). These measurements and their use play an important role in the development of validated, global, interactive earth system models being able to predict global climate and environmental change accurately enough to assist policy makers worldwide in making decisions concerning the protection and management of our environment and natural resources. The planned lifetime of these satellites is about 15 years. In case of satellite Terra, the first observations started in February 2000 and regular validated measurements are available from July 2000. In case of satellite Aqua, the validation process was shorter, so quality-controlled measurements are available from July 2002 (two months after the launch). The numerous climatic and environmental parameters are accessible via Internet at the Earth Observing System Data Gateway. Five instruments are included in satellite Terra (NASA, 1999): (1) ASTER (Advanced Spaceborne Thermal Emission and Reflection Radiometer), (2) CERES (Clouds and the Earth's Radiant Energy System), (3) MISR (Multi-Angle Imaging Spectroradiometer), (4) MODIS (Moderate Resolution Imaging Spectroradiometer), and (5) MOPITT (Measurements of Pollution in the Troposphere). Satellite Aqua carries the six following instruments: (1) MODIS (Moderate Resolution Imaging Spectroradiometer), (2) CERES (Clouds and the Earth's Radiant Energy System), (3) AIRS (Atmospheric Infrared Sounder), (4) AMSU-A (Advanced Microwave Sounding Unit), (5) HSB (Humidity Sounder for Brazil), and (6) AMSR-E - Advanced Microwave Scanning Radiometer for EOS.

The measurements of sensor MODIS from both satellites Terra and Aqua have been analyzed in this paper. MODIS measures biological and physical processes on the land and the ocean using a cross-track scanning multi-spectral radiometer with 36 electromagnetic spectral bands from visible to thermal infrared (Barnes et al., 1998). From the measurements of MODIS the following parameters are determined: surface temperature (both land and ocean), ocean color, global vegetation, cloud characteristics, snow cover, temperature and moisture profiles. MODIS is capable of viewing the entire globe daily at high resolution, namely 250 m per pixel in the visible and 1 km per pixel in the infrared channels.

In this paper, day-time and night-time surface temperature time series (with 1 km horizontal resolution) measured in the Central European region are analyzed. Surface temperature is strongly related to surface energy budget, especially, to latent and sensible heat flux. Calculation of surface temperature data is based on thermal infrared measurements of MODIS that are quality controlled and calibrated by surface observations (NASA, 1999). In order to determine the surface temperature output, seven spectral bands are used: 3660-3840 nm (channel 20), 3929-3989 nm (channel 22), 4020-4080 nm (channel 23), 8400-8700 nm (channel 29), 10780-11280 nm (channel 31), 11770-12270 nm (channel 32), and 13185-13485 nm (channel 33).

Wan and Snyder (1999) developed a model to calculate surface temperature from the spectral observations that can be applied in case of clear weather. This so-called Day/Night MODIS LST (Land Surface Temperature) Method is able to determine surface temperature and emissivity without preliminary knowing air temperature and water vapor profiles. The problem is underdetermined when we attempt to solve temperature and surface emissivity in  $N$  bands simultaneously solely from one-time observation (even if the exact atmospheric conditions are known). We have  $2N$  observations using one set during the day and another one during the night. The unknown variables are  $N$  bands emissivities, day-time surface temperature, night-time surface temperature, four atmospheric variables: air temperature and water vapor profiles during day and night, and the anisotropic factor;  $N+7$  altogether. So the radiation transfer equations can be solved if  $N \geq 7$ .

A linear approximation of the radiation transfer equation in the proximities of reference values of surface temperature and band emissivities results in a simplified form (Strahler et al., 1999). Combining 14 equations together ( $2 \times 7$  bands), the solution for surface temperature and band

emissivities should be a linear combination of the band brightness temperatures, each of which corresponds to one of the 14 observations.  $x_i$  can be written as follows:


$$x_i = \sum_{j=1}^{14} w_{i,j} \cdot y_j + w_{i,0} \quad (1)$$

where  $x$  is a vector of the 14 variables including surface temperature and band emissivities,  $y_j$  is the band brightness temperature for observation  $j$ ,  $w_{i,j}$  ( $i=1, \dots, 14$  and  $j=1, \dots, 14$ ) and  $w_{i,0}$  are the regression coefficients.

In order to separate urban and rural pixels, the MODIS Land Cover Product (LCP) have been used. These LCP values rely on a 1-km gridded database composited from different MODIS products, namely, land/water mask, albedo, spatial texture, directional reflectance, enhanced vegetation index, snow cover, land surface temperature, and terrain elevation information. These data are composited over a one-month time period to produce a globally consistent, multitemporal database on a 1-km grid as input to classification characterization algorithms. The LCP recognizes 17 categories of land cover following the International Geosphere-Biosphere Program scheme (Belward et al., 1999). Land cover classes are produced by processing the 32-day database using decision tree and artificial neural network classification algorithms to assign land cover classes based on training data (Strahler et al., 1999).

Since the topography significantly affects UHI, hilly regions have to be eliminated. To this process, the GTOPO30 global digital elevation model (DEM) has been used. This global data set was developed by the U.S. Geological Survey's (USGS) Earth Resources Observation System Data Center (USGS, 1996). The horizontal grid spacing of this database is 30-arc seconds (approximately 1 km). GTOPO30 is based on data derived from different sources of elevation information, e.g., Digital Terrain Elevation Data, USGS 1-degree DEM's, International Map of the World 1:1,000,000-scale maps, Digital Chart of the World (Danko, 1992).

Table 1. The geographical characteristics of the nine Central European cities used in this analysis. Latitude ( $\phi$ ) and longitude ( $\lambda$ ), height above sea level ( $h$ ), number of inhabitants ( $P$ ), and spatial extension ( $A$ ) are indicated.

	Name	$\phi$ (°N)	$\lambda$ (°E)	$h$ (m)	$P$ (persons)	$A$ (km <sup>2</sup> )
	Bucuresti	44.12°	26.57°	85	1 921 751	228
	Budapest	47.5°	19.05°	105	1 719 342	525
	Warsawa	52.17°	16.07°	100	1 692 854	525
	Vienna	48.12°	16.57°	183	1 598 626	415
	Milan	45.43°	9.28°	120	1 271 898	182
	Munich	48.15°	11.3°	310	1 247 873	519
	Sofia	42.5°	23.2°	564	1 138 950	215
	Beograd	44.82°	20.28°	117	1 120 092	198
	Zagreb	45.73°	16.07°	120	691 721	123

In the present analysis nine large cities from Central Europe (Table 1) with more than 1 million inhabitants (Brinkhoff, 2004) have been selected. Pixel representations of these selected urban agglomerations (including their rural environment) have been determined from a satellite image tile containing 1200×1200 pixels using sinusoid projection. Based on the spatial extension of the selected Central European cities, each urban agglomeration is represented by 50×50 pixels from the entire satellite image. The representative areas have been divided into urban and rural pixels in case of each city.

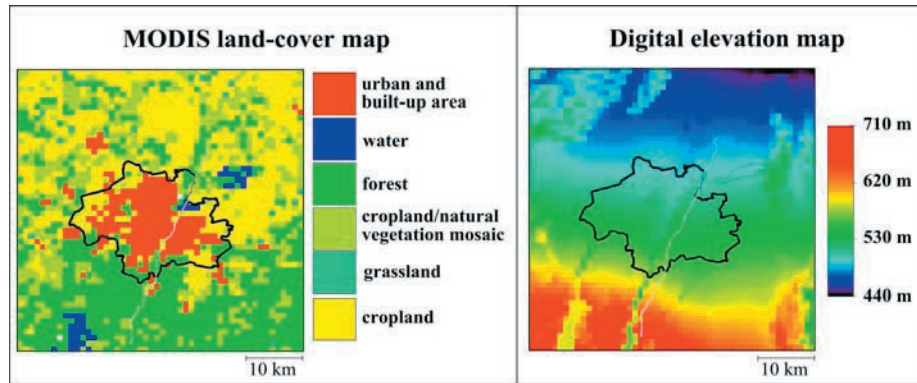


Fig. 1. The MODIS digital land-cover product (left panel) and the global digital elevation model (right panel) covering the Munich agglomeration area ( $50 \times 50 \text{ km}^2$ ) are used to separate urban and rural pixels of the region.

An example for Munich (located  $48.15^\circ\text{N}$ ,  $11.58^\circ\text{E}$  in Germany) is presented in Fig. 1. First, the MODIS LCP is applied to separate urban built-up and rural surrounding areas (left panel of Fig. 1). Urban part of the total area is defined within the 15-km radius circle around the city center. Rural pixels may be found within a 15-25-km radius ring around the city center. Furthermore, hilly regions have been eliminated using the global DEM (right panel of Fig. 1) when calculating the UHI intensity. Urban and rural pixels are within the  $\pm 50 \text{ m}$  and  $\pm 100 \text{ m}$  range of the city mean elevation value, respectively.

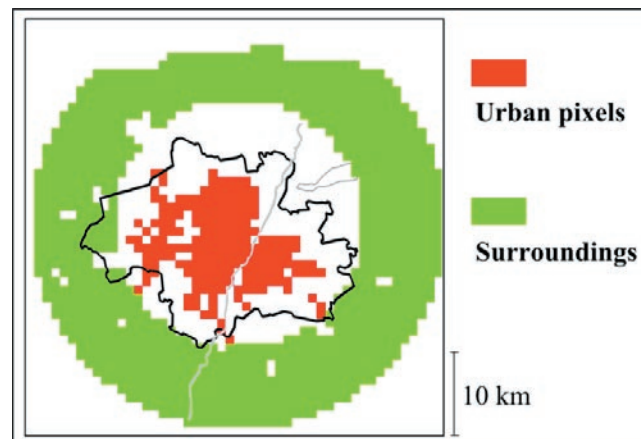


Fig. 2. Urban and rural pixels defined for the Munich agglomeration area.

The finally separated areas are demonstrated in Fig. 2 in case of Munich. Spatial averages of observed values converted to urban and rural surface temperature, UHI effects have been analyzed for the selected large cities located in different regions of Central Europe.

### 3. Results and discussion

In this section spatial structures of the UHI of several large cities located in Central Europe depending on seasons are analyzed and compared. Annual mean night-time UHI intensity is around  $2\text{--}3^\circ\text{C}$  as shown in Fig. 3, where the cities are ranked according to the number of their inhabitants (Brinkhoff, 2004). Basically, more populated cities exhibit more intense heat island. Orographical modification, distribution of land cover types of rural surroundings (i.e., portions of cropland,

grassland, and forest), and urban air quality disturb this relationship. Because of these effects UHI intensity is not exactly decreasing with less population.

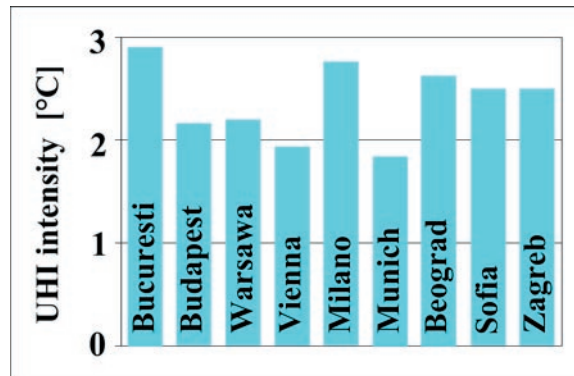


Fig. 3. Mean night-time UHI intensity of the nine selected cities in Central Europe. Annual mean values are determined using observations of the period 2001-2005.

Analyzing the 5-year-long time series of satellite-based observations (between 2001 and 2005) our results suggest that the annual variation of monthly mean UHI intensity is larger in day-time than in night-time. Fig. 4 illustrates this in case of four cities, i.e., Munich (located in Germany, 48.15°N, 11.58°E, 508 m above sea level), Warsaw (located in Poland, 52.25°N, 21.00°E, 107 m above sea level), Milan (located in Italy, 45.47°N, 9.20°E, 147 m above sea level), and Budapest (located in Hungary, 47.50°N, 19.08°E, 120 m above sea level). The most intense UHI effect occurs on summer days when monthly mean UHI is around 4-6°C. Direct solar radiation and thermal inertia can be considered as possible reasons. Based on the presented graphs, UHI intensity is larger in night-time than in day-time in the spring and autumn months, which is in contrast with the summer UHI intensities. This considerable difference can be explained partly by shorter day-time lengths in these equinox seasons than in summer, and partly by the relatively high values of air humidity and often occurring cloudy weather. Because of orographical effects (vicinity of the high Alps) night-time UHI of Milan in winter is more intense than day-time UHI.

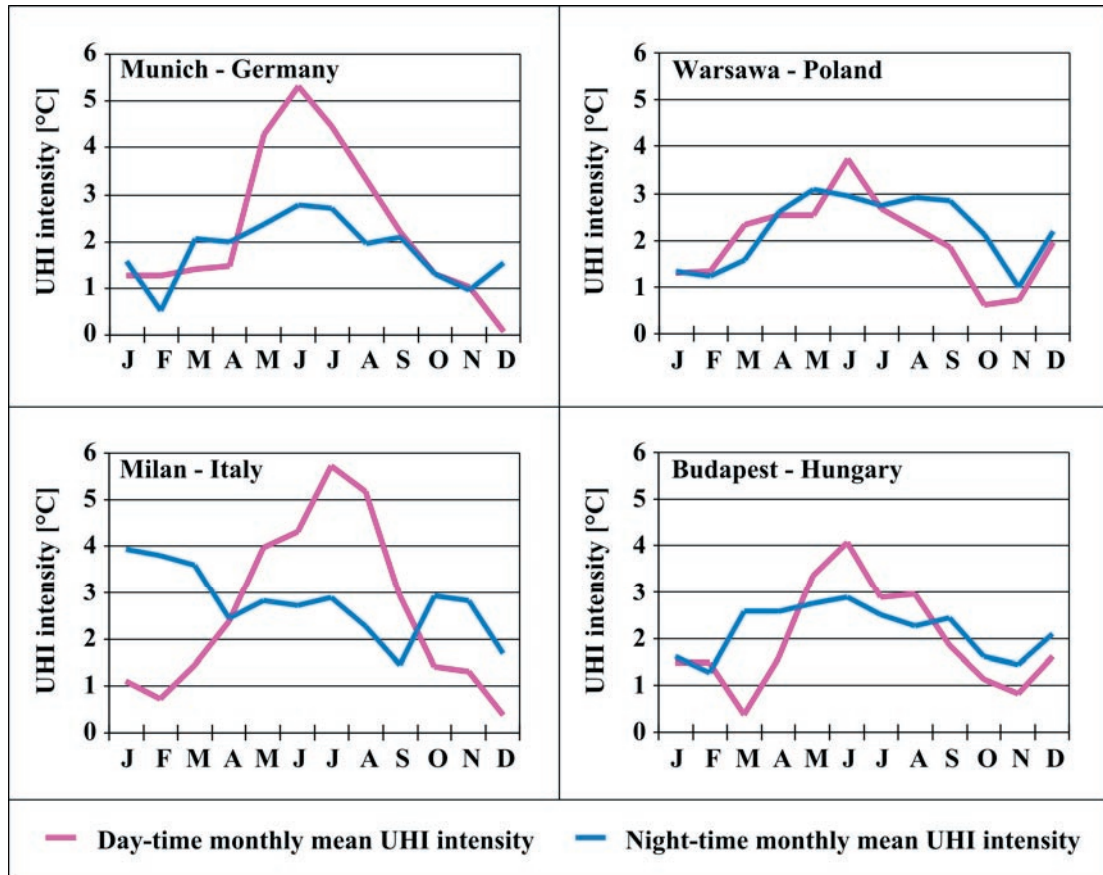


Fig. 4. Annual variation of monthly mean UHI intensity during day-time and night-time, 2001-2005.

Spatial structure of monthly mean UHI intensity of the nine selected agglomeration area in Central Europe has been analyzed in details. Fig. 5 illustrate the spatial structure of UHI in winter and summer in case of five cities during day-time (left panel) and night-time (right panel), respectively. The seasonal mean difference between the temperature of each pixel and the rural mean temperature is presented on the maps. The warmest part of each city is the downtown area (administrative and commercial center). In general, these downtown warm spots are 4-6°C and 2-3°C colder on winter days and nights, respectively, than in summer. The difference between the warmest and the coldest surface temperature exceeds 15°C in summer days where mountains are near the city (e.g., Budapest, Munich, Sofia). UHI in Sofia is very special, since Mountain Vitosa (2224 m) is located very close to the Bulgarian capital (mean elevation of Sofia is 550 m), that results in large temperature gradient within the selected rural area around the city, especially in summer. Summer day-time UHI structure of the Budapest agglomeration area is also unique (Pongrácz et al., 2006). The western part of the city is hilly covered by forests, so its surface is relatively cold. The downtown area (located on the left bank of the river Danube and characterized by 25-30 m high buildings from the late 19th century) can become very hot on summer days. The maximum difference between the warmest and the coldest surface temperature is about 10°C (occurring in summer) in case of the cities where the surroundings are less elevated and the orographical difference is less than 100 meter (e.g., Bucuresti, Warszawa).

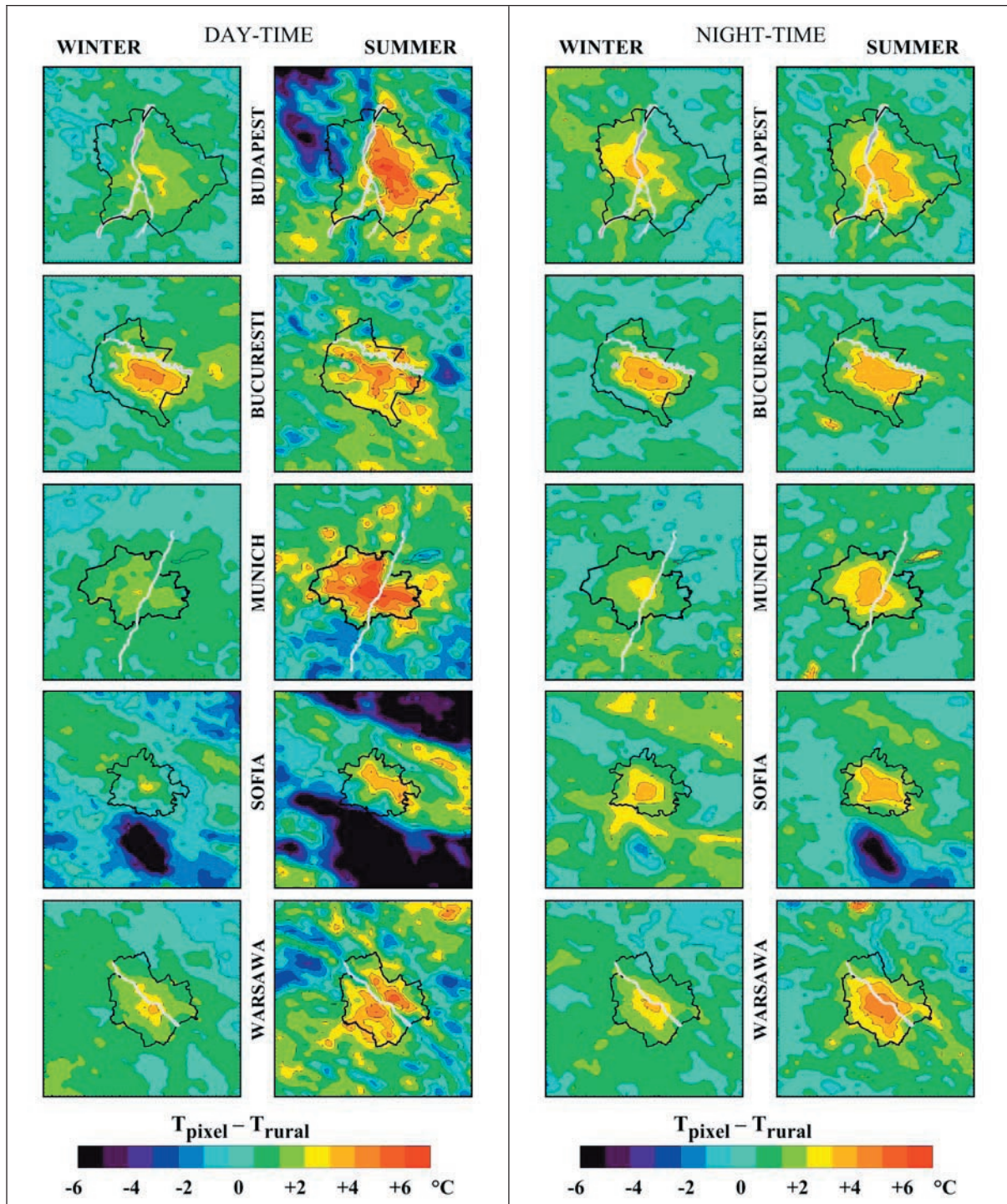


Fig. 5. Annual variation of monthly mean day-time (left panel) and night-time (right panel) UHI structure in Budapest, Bucuresti, Munich, Sofia, and Warsaw. MODIS surface temperature observed in 2001-2005 is used. Each map covers a  $50 \times 50 \text{ km}^2$  area.

In order to analyze the temporal variation of the UHI structure of the Central European agglomeration areas, time series of the monthly mean differences of surface temperature of each pixel and the rural mean along the major cross-sections (i.e., N-S, W-E, NW-SE, NE-SW) have been compared. In case of each city, the characteristic cross-section is selected and shown in Fig. 6. The selection is based on the representativeness of the geographical and orographical features of the cities and their surroundings.

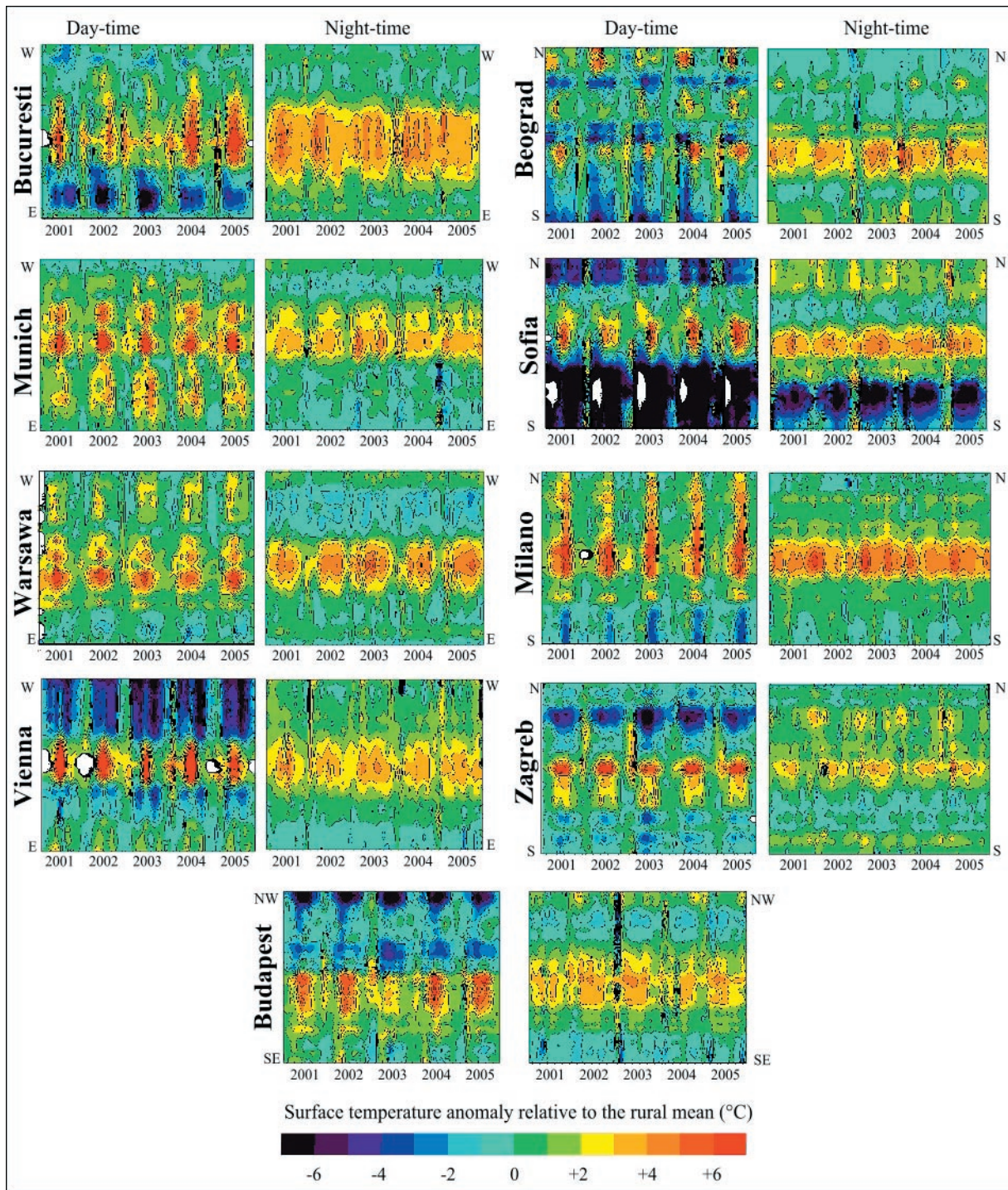


Fig. 6. Annual variation of monthly mean surface temperature in characteristic cross-sections of selected large cities from Central and Eastern Europe based on MODIS remote observations, 2001-2005.

The five-year-long time series (2001-2005) of day-time and night-time monthly mean surface temperature anomalies relative to the monthly rural means are calculated for each pixel in the 50×50 km<sup>2</sup> surrounding of the nine Central European cities from the MODIS observations. Left and right panel of Fig. 6 summarizes the time series of pixels located in the W-E (Bucuresti, Munich, Warsaw, Vienna) and the N-S (Beograd, Sofia, Milan, Zagreb) cross-sections of the selected regions,



respectively. In case of Budapest, the NW-SE cross-section represent the orographical variability of the city and the surroundings the most, therefore we selected this cross section (Dezső et al., 2006).

According to the results, the downtown regions can be clearly recognized due to the positive anomaly values that are greater than +5, +6°C, and +3, +4°C in day-time and night-time, respectively. Annual variation of the monthly means is more pronounced in day-time than in night-time, which was expected. The maximum anomaly occurs in summer months in both cases.

In order to accomplish a more detailed analysis of the energy balance of these large European agglomerations, very high-resolution satellite images may be used. For instance, another sensor of satellite Terra (i.e., ASTER) provides remotely sensed data with 90-m spatial resolution from July 2000. All these analyses may serve as a basis for urban planning and optimal selection of building materials.

#### 4. Conclusions

The UHI intensity has been analyzed in this paper using remotely sensed thermal information for nine populated Central European cities. First, these large agglomerations have been selected and their urban and rural pixel representations have been determined. Day-time and night-time surface temperature time series measured by the instrument MODIS of satellites Terra and Aqua have been analyzed. Urban and rural spatial means have been calculated and compared for each selected city. Based on the results presented in this paper the following conclusions can be drawn. (1) The UHI intensity detected in the selected Central European cities exhibits high variability. Monthly average values of the temperature differences between urban and rural areas range between 1°C and 6°C. Population of the cities (which is highly correlated with the industry) is the main factor of determining UHI intensity that is modified by orography. (2) Monthly mean spatial structures of UHI have been determined, concluding that the most intense UHI occurs in daytime in the summer period (May-June-July-August).

#### Acknowledgements

The authors thank NASA for producing the satellite surface temperature data in their present form and the Earth Observing System Data Gateway for distributing the data. Research leading to this paper has been supported by the Hungarian Academy of Sciences under the program 2006/TKI/246 titled Adaptation to climate change, the Hungarian National Science Research Foundation under grants T-034867, T-038423, and T-049824, also by the CECILIA project of the European Union Nr. 6 program under grant GOCE-037005, the Hungarian National Research Development Program under grants NKFP-3A/082/2004, and NKFP-6/079/2005, and VAHAVA project of the Hungarian Academy of Sciences and the Ministry of Environment and Water.

#### References

- Barnes, W.L., Pagano, T.S., Salamonson, V.V., 1998: Prelaunch characteristics of the Moderate Resolution Imaging Spectroradiometer (MODIS) on EOS-AM1. *IEEE Transactions on Geoscience and Remote Sensing*, 36, 1088-1100.
- Bartholy, J., Pongrácz, R., Dezső, Zs., 2001: Evaluation of urban heat island effect for large Hungarian cities using high resolution satellite imagery. In: *Proc. 5th European Conf. on Applications of Meteorology ECAM 2001*. Budapest.
- Belward, A.S., Estes, J.E., Kline, K.D., 1999: The IGBP-DIS 1-km land-cover data set DISCover: A project overview. *Photogram. Eng. Remote Sens.*, 65, 1013-1020.

- Brinkhoff, T. 2004: City population. <http://www.citypopulation.de>
- Carlson, T.N., Augustine, J.A., Boland, F.E., 1977: Potential application of satellite temperature measurements in the analysis of land use over urban areas. *Bull. Am. Meteorol. Soc.*, 58, 1301-1303.
- Danko, D.M., 1992: The digital chart of the world project. *Photogram. Eng. Remote Sens.*, 58, 1125-1128.
- Dezső, Zs., Bartholy, J., Pongrácz, R., 2005: Satellite-based analysis of the urban heat island effect. *Időjárás*, 109, 217-232.
- Howard, L., 1833: *Climate of London deduced from meteorological observations*. Vol. 1-3. Harvey and Darton.
- Matson, M., McClain, E.P., McGinnis, D.F., Pritchard, J.A., 1978: Satellite detection of urban heat island. *Mon. Wea. Rev.*, 106, 1725-1734.
- National Aeronautics and Space Administration (NASA), 1999: *Science writers' guide to Terra*. NASA Earth Observing System Project Science Office.
- Oke, T.R., 1973: City size and the urban heat island. *Atmospheric Environment*, 7, 769-779.
- Oke, T.R., 1982: The energetic basis of the urban heat island. *Q.J.R. Meteorol. Soc.*, 108, 1-24.
- Pongrácz, R., Bartholy, J., Dezső, Zs., 2006: Remotely sensed thermal information applied to urban climate analysis. *Advances in Space Research*, 37, 2191-2196, DOI: 10.1016/j.asr.2005.06.069
- Price, J.C., 1979: Assessment of the heat island effect through the use of satellite data. *Mon. Wea. Rev.*, 107, 1554-1557.
- Rao, P.K., 1972: Remote sensing of urban heat islands from an environmental satellite. *Bull. Am. Meteorol. Soc.*, 53, 647-648.
- Roth, M., Oke, T.R., Emery, W.J., 1989: Satellite-derived urban heat island from three coastal cities and the utilization of such data in urban climatology. *Int. J. Remote Sensing*, 10, 1699-1720.
- Sokhi, R.S., Ed. 1998: *Urban air quality: monitoring and modelling*. Kluwer. 351p.
- Strahler, A., Muchoney, D., Borak, J., Friedl, M., Gopal, S., Lambin, E., Moody, A., 1999: MODIS land cover product algorithm theoretical basis document, version 5.0. Center for Remote Sensing, Dept. of Geography, Boston University.
- Sundborg, A., 1950: Local climatological studies of the temperature conditions in an urban area. *Tellus*, 2, 222-232.
- United States' Geological Survey (USGS), 1996: *GTOPO30 documentation*. USGS.
- Unger, J., Sümeghy, Z., Zoboki, J., 2001: Temperature cross-section features in an urban area. *Atmospheric Research*, 58, 117-127.
- Wan, Z., Snyder, W., 1999: MODIS land-surface temperature algorithm theoretical basis document. Inst. for Computational Earth Systems Science, Univ. of California.